A Simple Technique for the Design of MMIC 90° Phase-Difference Networks

Mustapha Mahfoudi and José I. Alonso, *Member, IEEE*

Abstract— **In this paper, a simple technique for the design of broadband 90° phase-difference networks, using balanced and unbalanced all-pass network topologies, is presented. In the developed method, the element values of the structures are calculated as function of two design variables: Q_0 and r. Utilizing this approach, a 90° phase shifter has been realized, having less than 2° phase error and better than 0.5 dB amplitude error in the operating band from 0.7 to 3.5 GHz.**

I. Introduction

As GaAs microwave monolithic integrated circuit (MMIC) technology advances, the need of basic building blocks has become evident. On the other hand, this technology allows the placing of components at small distances one from another and, so on, they can be considered as composed of lumped elements in high operational frequencies. This new alternative approach of designing microwave circuits make possible to realize monolithic versions of old theoretical circuits proposed long time ago.

One of this key circuits are those which allow to have a constant phase difference at their output over a band of frequencies. These networks have been used for the realization of active power splitters [1], 90° phase shifters [2], and as circuits for generation of multiple phase coherent signals [3]–[5], which can be an integrated part of single side-band modulators [6], frequency-shift keying systems [7], direct-quadrature modulators [8]–[9], and beam-forming networks [10].

This paper deals with the design and realization of broadband 90° phase difference networks, utilizing balanced and unbalanced all-pass networks topology. The basic configuration of a phase-difference network consist of two all-pass filters, which inputs are driven in parallel. The phase difference between their outputs constitute the output of the phase shifter.

Although the theoretical background for the design of all-pass networks whose output phase difference is constant over a prescribed frequency band is well known and is perfectly covered in the literature [11]–[14], its application is cumbersome and ambiguous with regard to calculate the circuit element values to obtain 90° phase difference.

Therefore, from a practical point of view of monolithic implementation of this kind of networks, it would be desirable to develop a method which permit to obtain the element values as function of design parameters, normally, the relative bandwidth and the phase difference.

Manuscript received October 17, 1995; revised June 14, 1996. This work was supported in part by Project TIC93-005-C03-01 of National Board of Scientific and Technological Research (CICYT) and by the International Cooperation Spanish Agency (AECI).

The authors are with the Departamento Señales, Sistemas y Radiocomunicaciones, ETSI Telecomunicación, Universidad Politécnica de Madrid, Ciudad Universitaria, Madrid, Spain.

Publisher Item Identifier S 0018-9480(96)06905-0.

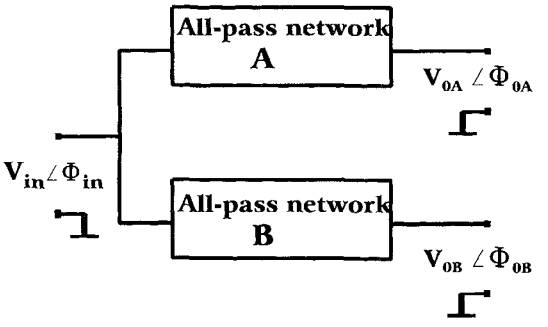

Fig. 1. Phase-difference network using all-pass filter.

In the design method developed for designing 90° phase difference networks, based on second-order all-pass filters, two design parameters r and Q_0 have been chosen. The element values of several circuital configurations that have been studied, can be calculated as function only of these variables, which are in his turn depending on a design variable: the ratio of the low to high frequency of operational band.

Special emphasize is made on the RC all-pass filters because this option reveals yielding wider shift band, small size, lower power and high reliability and therefore most suitable for monolithic implementation.

II. Second Order All-Pass Filters

As it has been pointed out, two all-pass filters connected as shown in Fig. 1, can be designed to have a phase difference between their output voltages approximate to a constant over a band of frequencies.

First, a classification of all-pass filters which constitute the phase difference networks, in two main categories, namely, passive and active all-pass networks, is proposed. Second, the general properties of the complete circuit are discussed and a simple design method for second-order all-pass filters is proposed.

A. Passive All-Pass Filters

The general structure is shown in Fig. 2. These balanced structures results in a complex circuitry because of additional stages must be included in order to achieve a balanced signal from the single-ended input. However, they have been used in many applications which require integration with balanced input circuits [4]–[5].

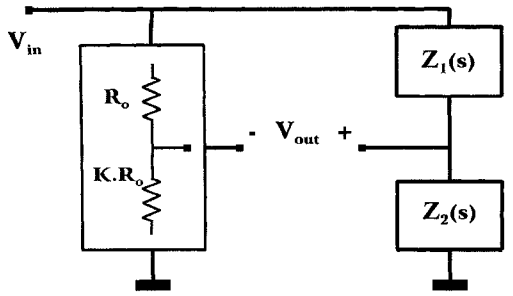

Fig. 2. General structure of passive all-pass networks.

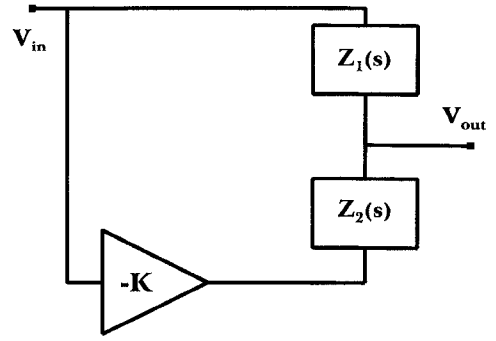

Fig. 3. General structure of active all-pass networks (Type I).

Although, the two impedance functions $Z_1(s)$ and $Z_2(s)$ can contain resistors, capacitors and inductors, however, normally only RC passive all-pass filters are realized in monolithic technology, although the RC configuration will result in higher transmission losses.

B. Active All-Pass Filters

Two general structures for active all-pass filters have been identified. The circuit structure shown in Fig. 3, will be sensible to the impedance presented at its output, while the second structure, depicted in Fig. 4, will be not. The active networks have several advantages as contrasted with passive configurations. They are single-ended circuits, have not transmission losses and they have the possibility of adjustment offered by the active element, which can be useful in some applications.

C. General All-Pass Transfer Function

For the three general configurations, the transfer function can be written as

$$T(s) = \frac{V_{\text{out}}}{V_{\text{in}}} = G \cdot \frac{Z_2(s) - K \cdot Z_1(s)}{Z_2(s) + Z_1(s)} = G \cdot \frac{N_1(s)}{N_2(s)} \quad (1)$$

where s is the complex frequency and G is a constant. The two branch impedances $Z_1(s)$ and $Z_2(s)$ along with the K parameter are chosen so that $T(s)$ is an all-pass function. A rational function is an all-pass one when the numerator and denominator polynomials accomplish the property

$$N_1(s) = N_2(-s). \quad (2)$$

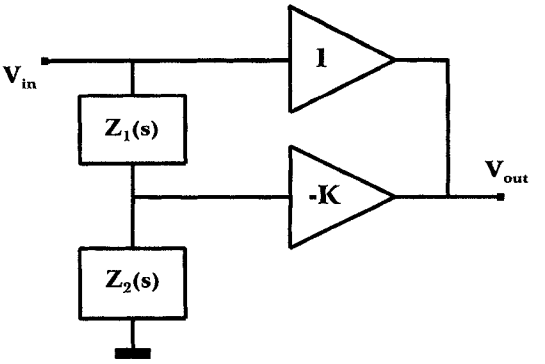

Fig. 4. General structure of active all-pass networks (Type II).

Therefore, the second-order transfer function $T(s)$ can be written in a general form as

$$T(s) = \frac{V_{\text{out}}}{V_{\text{in}}} = G \cdot \frac{s^2 - a_1 s + a_0}{s^2 + a_1 s + a_0} = G \cdot \frac{s^2 - \frac{\omega_0}{Q_0} s + \omega_0^2}{s^2 + \frac{\omega_0}{Q_0} s + \omega_0^2} \quad (3)$$

where a_0 and a_1 are real coefficients, ω_0 is the characteristic frequency and Q_0 the characteristic Q.

To understand how all-pass filters are used to built up phase shifters, we obtain the physical frequency behavior of $T(s)$ by letting $s = j\omega$ and evaluating $T(s)$ along the imaginary axis. Thus

$$T(j\omega) = G \cdot \frac{\omega_0^2 - \omega^2 - j\frac{\omega_0 \omega}{Q_0}}{\omega_0^2 - \omega^2 + j\frac{\omega_0 \omega}{Q_0}} = G \cdot \frac{1 + jQ_0\left(\frac{\omega_0}{\omega} - \frac{\omega}{\omega_0}\right)}{1 - jQ_0\left(\frac{\omega_0}{\omega} - \frac{\omega}{\omega_0}\right)} \quad (4)$$

so the phase of the voltage transfer function can be written as

$$\Phi(\omega_0, Q_0) = 2 \cdot \tan^{-1}\left[Q_0\left(\frac{\omega_0}{\omega} - \frac{\omega}{\omega_0}\right)\right]. \quad (5)$$

The phase characteristic, given by the previous expression, is plotted against relative frequency $-\omega/\omega_0$—for different values of Q_0 in Fig. 5. It is seen that Q_0 controls the general shape of the phase curve, while the frequency characteristic ω_0 locates the curve on a logarithmic frequency scale, without altering its form. The linear region of the phase curve occurs over a frequency range centred in ω_0 and its length depends on Q_0 value. For values comprised between the two indicated ones on the plot, the linear region occurs over a wide frequency range. In other hand, from (3) the amplitude G is a constant for all frequencies and it is independent of Q_0 and ω_0 parameters. So, we can obtain two all-pass networks of the same G value and different Q_0 and ω_0 parameters. The discussed properties are used to built up phase shifters based on the all-pass networks.

III. Phase Shifter Design

Let consider a pair of all-pass networks, noted A and B, as is shown in Fig. 1. In accordance with (5) the phase transfer functions of each individual network can be written as

$$\Phi_{0A} = 2 \cdot \tan^{-1} Q_A\left(\frac{f_A}{f} - \frac{f}{f_A}\right)$$

and

$$\Phi_{0B} = 2 \cdot \tan^{-1} Q_B\left(\frac{f_B}{f} - \frac{f}{f_B}\right) \quad (6)$$

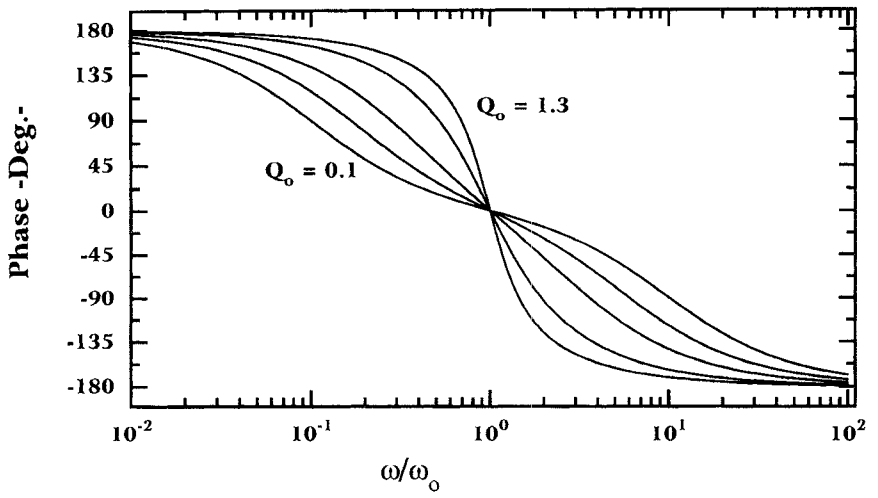

Fig. 5. Phase characteristics of second-order all-pass networks versus normalized frequency.

where Q_A, f_A, Q_B, f_B are, respectively, the characteristic Q and characteristic frequency of networks A and B.

In accordance with the previous section, it can be proved that when the two parameters Q_A and Q_B have a same value, the two phase curves, Φ_{0A} and Φ_{0B}, will have the same aspect versus frequency, and their linear parts are parallel and aparted from each others by a quantity of $\omega_B - \omega_A$. In order to represent mathematically the phase difference construction, we introduce two new parameters: f_0 and r, defined as follows:

$$f_0^2 = f_A \cdot f_B \quad \text{and } r^2 = \frac{f_B}{f_A}. \tag{7}$$

In terms of these new parameters and considering that $Q_A = Q_B = Q_0$, the phase-difference function of their outputs, can be expressed as follows:

$$\begin{aligned}\Phi(f) &= \Phi_{0A} - \Phi_{0B} \\ &= 2 \cdot \tan^{-1} Q_0 \left(\frac{f_0}{r \cdot f} - \frac{r \cdot f}{f_0} \right) \\ &\quad - 2 \cdot \tan^{-1} Q_0 \left(\frac{r \cdot f_0}{f} - \frac{f}{r \cdot f_0} \right).\end{aligned} \tag{8}$$

In this way, the design parameters are r, f_0 and Q_0. The design approach presented in this paper, allows to obtain these parameters as function of frequency band, in order to approximate this difference to 90°. On the other hand, the amplitude ratio can easily made equal to 1 by choosing the constants G_A and G_B equals.

IV. Systematic Design

A. General Phase Difference Expression

When 90° phase difference is needed, the expression (8) is solved for $\Phi(f) = 90°$ and Q_0 and r parameters can been easily found. This is done at a single frequency and it gives zero phase error at that specified frequency. However, apart from this frequency the phase error rise rapidly, so this design procedure is not optimum for a wideband design. As it will be shown, for each frequency range defined by its lower frequency edge $f_{\min}$ and the upper one $f_{\max}$, it corresponds a unique parameter couple (Q_0, r) which make the phase difference close to 90° all over these range, minimizing the phase error within it.

In order to apply a systematic approach design to any desired frequency range $(f_{\min}, f_{\max})$, a simple design method has been developed. In the method proposed, the Q_0 and r design parameters are obtained by substitution of $f_{\min}$ and $f_{\max}$ variables in a closed form expression. The elements values of proposed structures can be easily calculated, because these are expressed as function of these design parameters.

The (8) can be rewritten in the following form

$$\Phi(f) = 2 \tan^{-1} \left\{ \frac{\frac{1}{Q_0}\left(r - \frac{1}{r}\right)\left(\frac{f}{f_0} + \frac{f_0}{f}\right)}{\frac{1}{Q_0^2} - \left(r - \frac{1}{r}\right)^2 - 4 + \left(\frac{f}{f_0} + \frac{f_0}{f}\right)^2} \right\}. \tag{9}$$

It can be easily shown that the phase difference function has an even symmetry on f about f_0 and an odd symmetry on r about $r = 1$ in a logarithmic scale. This equation represents the general phase-versus-frequency characteristic of the complete network and it is similar to that presented in [11], however, the latter formulation is quite arbitrary. In the following we give the steps and criterions used in the technique developed to derive Q_0 and r closed form expressions.

B. 90° Phase Difference Computation

If the phase difference function is set to 90° at the centre frequency $f = f_0$, that is to say, $\Phi_0 = \Phi(f = f_0) = 90°$, a relation between the parameters Q_0 and r can be established. This relationship is given by the next equation

$$\left(r - \frac{1}{r}\right)^2 + \frac{2}{Q_0}\left(r - \frac{1}{r}\right) - \frac{1}{Q_0^2} = 0. \tag{10}$$

The previous equation is a second-order equation on $(r - \frac{1}{r})$ variable which solution is given by

$$\left(r - \frac{1}{r}\right) = \frac{1}{Q_0}(-1 \pm \sqrt{2}). \tag{11}$$

With Q_0 and r related through (11), the phase difference curve is plotted in Fig. 6 against the relative frequency with Q_0

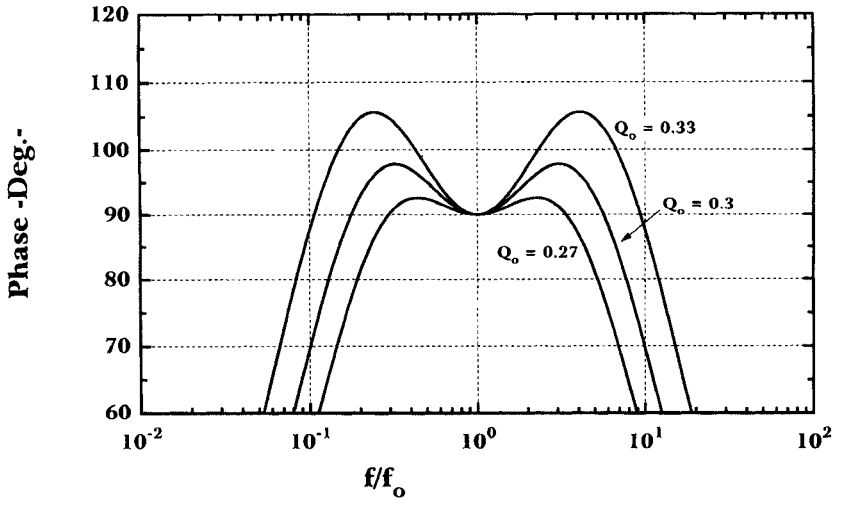

Fig. 6. Phase shift of a second-order all-pass network.

as parameter. Must be taken in mind that the two r solutions of (11) give the same Φ curve since its symmetry property. The phase difference is exactly 90° at f_0 and, depending on Q_0 value, the phase difference can cover different frequency bandwidths around f_0 width a corresponding error ripple.

C. Minimum Phase Shift Error Criterions

Given a frequency bandwidth, a Q_0 value should be chosen to minimize the phase shift error within it. The criterion used to get a compromise between the phase shift error and the operating bandwidth is based on the fact that for the same band and the same phase difference shape (so the same Q_0 value) minimum error is obtained making Φ_0 slightly different from 90° in such away that the two maximums and the minimum (Φ_0) are apart from 90° with the same amount, this is traduced to the following expression

$$\Phi_0 + \frac{\Phi_{\max} - \Phi_0}{2} = 90°. \tag{12}$$

In (12) Φ_0 is find out from (9) by the substitution of f_0 for f and $\Phi_{\max}$ is computed in Appendix A. Its value is given by

$$\Phi_{\max} = 2 \cdot \tan^{-1}\left\{\frac{1}{2}\frac{1}{Q_0}\left(r - \frac{1}{r}\right) \times \left[\frac{1}{Q_0^2} - \left(r - \frac{1}{r}\right)^2 - 4\right]^{-\frac{1}{2}}\right\}. \tag{13}$$

Rewriting (12) gives

$$\tan\frac{\Phi_0}{2} = \frac{1}{\tan\frac{\Phi_{\max}}{2}}. \tag{14}$$

Replacing Φ_0 and $\Phi_{\max}$ in (14) and rearranging terms the following equation on Q_0 and r is obtained

$$\frac{1}{Q_0^2}\left(r - \frac{1}{r}\right)^2 = \left[\frac{1}{Q_0^2} - \left(r - \frac{1}{r}\right)^2\right]\sqrt{\frac{1}{Q_0^2} - \left(r - \frac{1}{r}\right)^2 - 4}. \tag{15}$$

This relation replace the one used in (11) to compute the phase shift difference, further to do this, the latter minimizes the phase shift error. Since two parameters are implicated a second relation is needed to set the correspondence between $(f_{\min}, f_{\max})$ and (Q_0, r). This relation is derived from the fact that the ripple of phase curves is set to be constant over the whole frequency band. At the edges $f_{\max}$ and $f_{\min}$ we have

$$\Phi(f = f_{\max}) = \Phi(f = f_{\min}) = \Phi_0 \tag{16}$$

and from (9) and (10) we get

$$\frac{\frac{1}{Q_0}\left(r - \frac{1}{r}\right)\left(\frac{f_{\max}}{f_0} + \frac{f_0}{f_{\max}}\right)}{\frac{1}{Q_0^2} - \left(r - \frac{1}{r}\right)^2 - 4 + \left(\frac{f_{\max}}{f_0} + \frac{f_0}{f_{\max}}\right)^2} = \frac{\frac{2}{Q_0}\left(r - \frac{1}{r}\right)}{\frac{1}{Q_0^2} - \left(r - \frac{1}{r}\right)^2}. \tag{17}$$

At this stage a new parameter R is introduced to characterize the frequency bandwidth. R is defined as $R^2 = \frac{f_{\max}}{f_{\min}}$ and $f_0^2 = f_{\max} f_{\min}$. In terms of this parameter, the (17) leads to the following relation

$$\frac{1}{Q_0^2} - \left(r - \frac{1}{r}\right)^2 = 2\left(R + \frac{1}{R} + 2\right) \tag{18}$$

replacing (18) into (15) gives the Q_0 and r final solutions

$$\left(r - \frac{1}{r}\right)^2 = \left(R + \frac{1}{R} + 2\right)\left[\sqrt{1 + \frac{2\sqrt{2}\sqrt{R + \frac{1}{R}}}{R + \frac{1}{R} + 2}} - 1\right]$$

$$\frac{1}{Q_0^2} = \frac{2\sqrt{2}\sqrt{R + \frac{1}{R}}}{\sqrt{1 + \frac{2\sqrt{2}\sqrt{R + \frac{1}{R}}}{R + \frac{1}{R} + 2}} - 1}. \tag{19}$$

Fig. 7 shows the plot of Q_0 and r against $f_{\max}/f_{\min}$, for a given bandwidth. The design parameters are computed from (19) or directly read from the plot of Fig. 7.

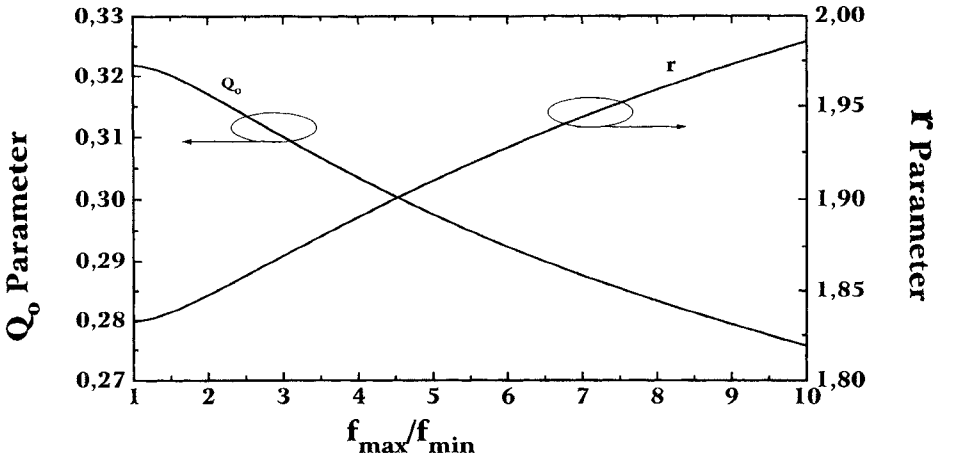

Fig. 7. Design parameters (Q_0, r) versus frequency bandwidth.

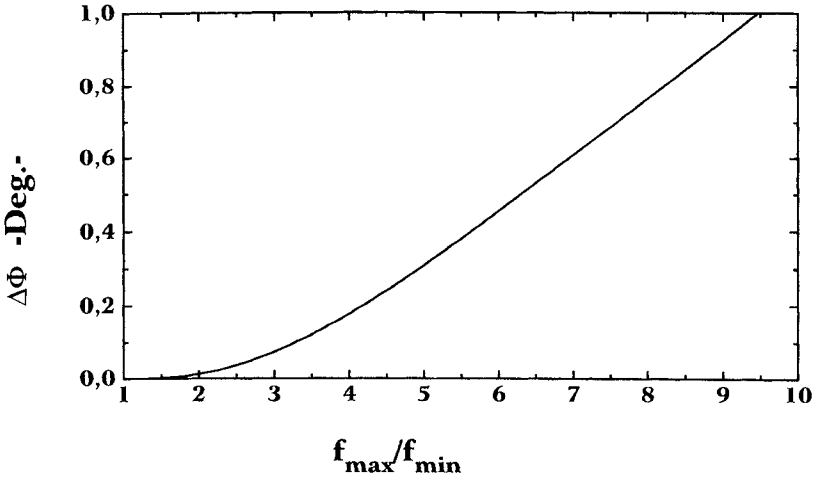

Fig. 8. Phase shift error versus frequency bandwidth.

D. Phase Shift Performance

The phase shift error $\Delta\Phi$ expression is

$$\Delta\Phi = \Phi_{\max} - 90^\circ = 90^\circ - \Phi_0 \tag{20}$$

$$\Delta\Phi = 90^\circ - 2\tan^{-1}\left\{\frac{\frac{2}{Q_0}\left(r - \frac{1}{r}\right)}{\frac{1}{Q_0^2} - \left(r - \frac{1}{r}\right)^2}\right\}. \tag{21}$$

Equation (21) is plotted in Fig. 8 versus relative bandwidth. As is shown large bandwidth phase shift with small error operation is obtained.

E. Design Diagram

The two design parameters determine the analytical expressions of the two transfer functions $T_A(j\omega)$ and $T_B(j\omega)$. On other hand, by the synthesis of this functions a relationship between the design parameters and the circuit elements can be easily stablished. So, the element values can be computed as functions of Q_0 and r parameters.

The design sequence is resumed in the diagram of Table I.

TABLE I
90° PHASE SHIFTER DESIGN DIAGRAM

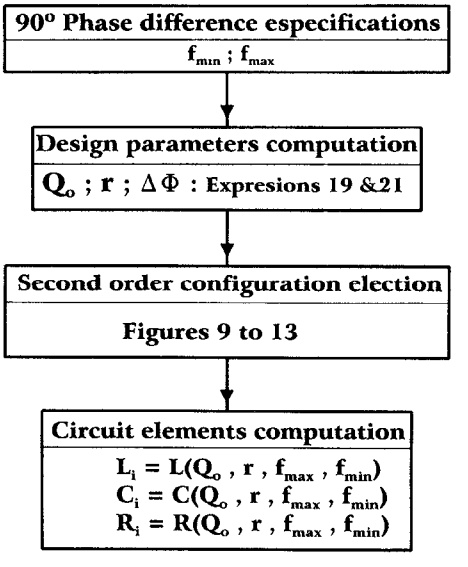

V. PROPOSED PHASE SHIFTER DESIGNS

Different passive all-pass structures to be designed using the described method are shown in Figs. 9–11. The design

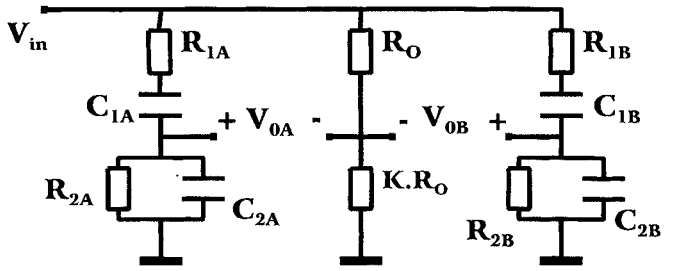

$$R_{1A} = \frac{r}{2\pi\sqrt{f_{max} \cdot f_{min}}} \frac{1}{C_{1A}} \qquad R_{1B} = \frac{1}{2\pi r\sqrt{f_{max} \cdot f_{min}}} \frac{1}{C_{1B}}$$

$$R_{2A} = \frac{r\left(\frac{1}{Q_o} - 2\right)}{2\pi\sqrt{f_{max} \cdot f_{min}}} \frac{1}{C_{1A}} \qquad R_{2B} = \frac{\left(\frac{1}{Q_o} - 2\right)}{2\pi r\sqrt{f_{max} \cdot f_{min}}} \frac{1}{C_{1B}}$$

$$C_{2A} = \frac{C_{1A}}{\left(\frac{1}{Q_o} - 2\right)} \qquad C_{2B} = \frac{C_{1B}}{\left(\frac{1}{Q_o} - 2\right)}$$

$$G_o = \frac{1}{2}(1 - 2Q_o) \qquad K = \frac{1 - 2Q_o}{1 + 2Q_o}$$

Fig. 9. Schematic and design equations of a passive phase shifter, with resistors and capacitors (Type I).

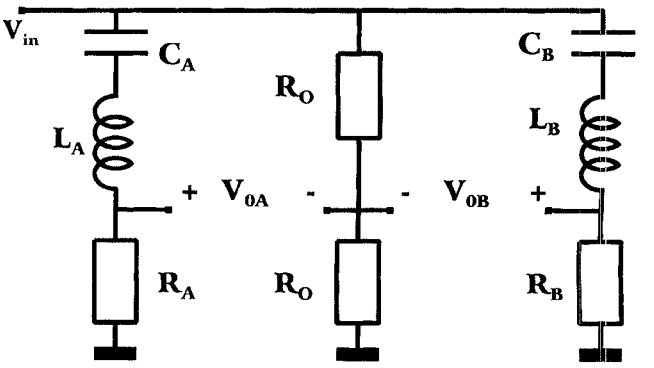

$$C_A = \frac{r^2}{4\pi^2 L_A f_{max} f_{min}} \qquad C_B = \frac{1}{4\pi^2 L_B r^2 f_{max} f_{min}}$$

$$R_A = \frac{2\pi\sqrt{f_{max} f_{min}}\, L_A}{r Q_o} \qquad R_B = \frac{2\pi\sqrt{f_{max} f_{min}}\, L_B r}{Q_o}$$

$$G_o = \frac{1}{2} \qquad R_o\ ;\ L_A\ ;\ L_B$$

Fig. 10. Schematic and design equations of a passive phase shifter, with inductors and capacitors (Type II).

procedure to calculate the components is similar to that presented in [9]. For each structure the relationships between the circuit components and design parameters are also given inset. Implementations of the two active structures is given in Figs. 12 and 13. For practical considerations, the active stage can be implemented as a common source MESFET amplifier, in the special case where $K = 1$, a differential amplifier may be used.

In the structure of Fig. 9, two capacitor elements C_{1A} and C_{1B} are elected independently of the phase shifter specifications. The same occurs with the elements L_A and L_B in Figs. 10 and 11. Since these elements scale all the others circuit elements, the convenient criterion to fix their values is to do meet the specified circuit impedance level, or to make all the circuit elements realizable in monolithic technology. The later criterion is particularly useful in the inductors case. In Figs. 12 and 13, the resistors R_{2A} and R_{2B} and the capacitors C_{2A} and C_{2B} are designed as the active stages output impedance and input impedance, respectively.

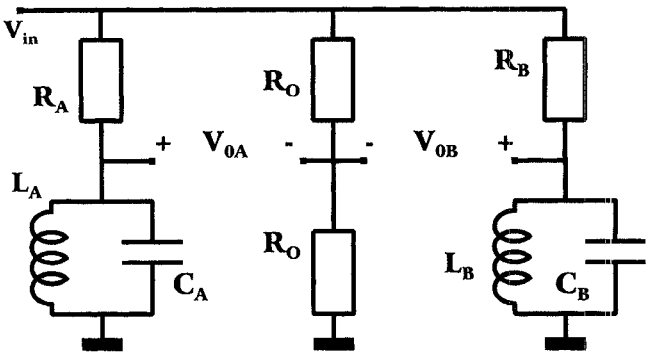

$$C_A = \frac{r^2}{4\pi^2 L_A f_{max} f_{min}} \qquad C_B = \frac{1}{4\pi^2 L_A r^2 f_{max} f_{min}}$$

$$R_A = \frac{2\pi\sqrt{f_{max} f_{min}}\, L_A Q_o}{r} \qquad R_B = 2\pi\sqrt{f_{max} f_{min}}\, L_B r Q_o$$

$$G_o = \frac{1}{2} \qquad R_o\ ;\ L_A\ ;\ L_B$$

Fig. 11. Schematic and design equations of a passive phase shifter,with inductors and capacitors (Type III).

VI. Example: An Active 90° Phase Shifter Realization

To check the validity of the proposed design approach a phase shifter circuit corresponding to the active structure of Fig. 12 has been realized and measured to operate over the frequency range 0.6–3.5 GHz. The objective was to achieve state of the art performance of the active type, since RC passive realization has been already reported [4]. The design and performance of the phase shifter corresponding to the Fig. 13 are similar in most aspects.

Since $f_{min} = 0.6$ GHz and $f_{max} = 3.5$ GHz, from Fig. 8 the theoretic phase error is 0.5° and from Fig. 7, $r = 1.9$ and $Q_0 = 0.3$. The calculated component values are

$$R_{2A} = 120.0\ \Omega \quad R_{2B} = 162.0\ \Omega$$
$$R_{1A} = 159.7\ \Omega \quad R_{1B} = 215.8\ \Omega$$
$$C_{1A} = 0.82\ \text{pF} \quad C_{1B} = 0.026\ \text{pF}$$
$$C_{2A} = 1.10\ \text{pF} \quad C_{2B} = 0.36\ \text{pF}.$$

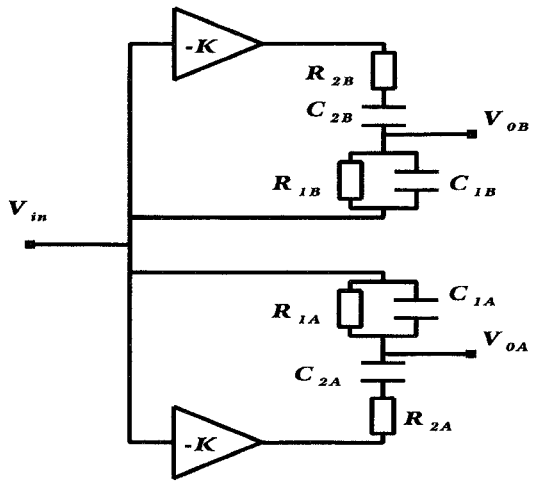

$$R_{1A} = \left(\frac{1}{Q_o} - 2\right) R_{2A} \qquad R_{1B} = \left(\frac{1}{Q_o} - 2\right) R_{2B}$$

$$C_{1A} = \frac{r}{2\pi\sqrt{f_{max} \cdot f_{min}}\left(\frac{1}{Q_o} - 2\right)} \frac{1}{R_{2A}} \qquad C_{1B} = \frac{1}{2\pi r\sqrt{f_{max} \cdot f_{min}}\left(\frac{1}{Q_o} - 2\right)} \frac{1}{R_{2B}}$$

$$C_{2A} = \frac{r}{2\pi\sqrt{f_{max} \cdot f_{min}}} \frac{1}{R_{2A}} \qquad C_{2B} = \frac{1}{2\pi r\sqrt{f_{max} \cdot f_{min}}} \frac{1}{R_{2B}}$$

$$G_o = 1 \qquad K = \frac{1 + 2Q_o}{1 - 2Q_o}$$

Fig. 12. Schematic and design equations of an active phase shifter (Type I).

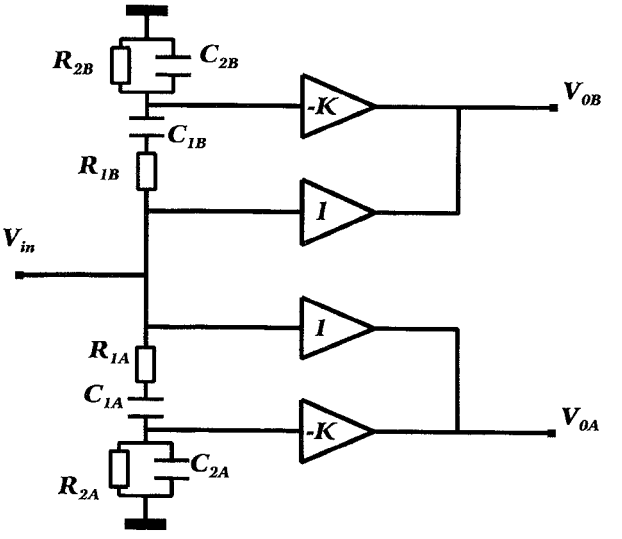

$$C_{1A} = \left(\frac{1}{Q_o} - 2\right) C_{2A} \qquad C_{1B} = \left(\frac{1}{Q_o} - 2\right) C_{2B}$$

$$R_{1A} = \frac{r}{2\pi\sqrt{f_{max} \cdot f_{min}}\left(\frac{1}{Q_o} - 2\right)} \frac{1}{C_{2A}} \qquad R_{1B} = \frac{1}{2\pi r\sqrt{f_{max} \cdot f_{min}}\left(\frac{1}{Q_o} - 2\right)} \frac{1}{C_{2B}}$$

$$R_{2A} = \frac{r}{2\pi\sqrt{f_{max} \cdot f_{min}}} \frac{1}{C_{2A}} \qquad R_{2B} = \frac{1}{2\pi r\sqrt{f_{max} \cdot f_{min}}} \frac{1}{C_{2B}}$$

$$G_o = 1 \qquad K = \frac{2}{1 - 2Q_o}$$

Fig. 13. Schematic and design equations of an active phase shifter (Type II).

The gain of the active stage is $K = 12$ dB. It has been implemented as a common source 0.5 μm-gate-length MESFET. The two outputs are fed to a pair of source followers which act to buffer the circuit from varying the presented load impedance. The schematic of the circuit is shown in Fig. 14. The resistors R_{2A} and R_{2B} are simulated as the active stage output resistances.

A chip photograph is shown in Fig. 15. It has been designed to be fully on-wafer testable. All measurements were done on wafer using coplanar RF probes. The chip has been manufactured using the 0.5-μm F20 process of GEC-Marconi, which includes two metal levels and via holes. The chip area is 1100×2200 μm^2, and it contains 4 MESFET transistors, 8 resistors and 2 capacitors. The layout has been simulated with the LIBRA simulation program of HP-Eesof. Figs. 16 and 17 show the simulated and measured performances, resulting in 2.5° maximum phase shift error and 0.5 dB maximum amplitude ratio error over the whole frequency range 0.6–3.5 GHz. The dc bias provides a precise tuning of the phase shift and amplitude ratio errors to 0.5° and 0.1 dB for 200 MHz bands within the range 0.6–3.5 GHz.

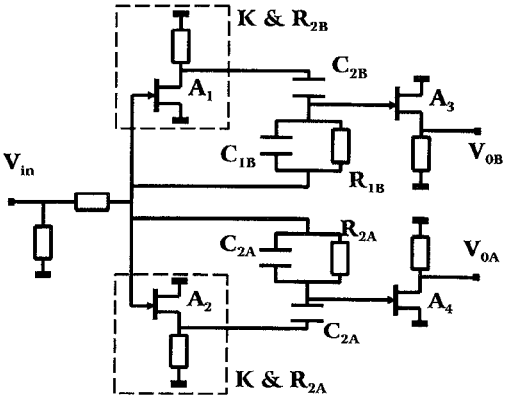

Fig. 14. Circuit schematic.

VII. Conclusion

The overall paper is intended to simplify the design of phase shifters at microwave frequency using GaAs MMIC technology. An accurate unified method for calculating the component values for a variety of all pass 90° phase shifter configurations has been presented. These configurations are thought for easy MMIC integration. To prove the proposed approach an 90° active phase shifter has been implemented. Small phase shift error and amplitude error have been measured over more than two octaves bandwidth. The dc bias give a fine tuning and adjustment of the circuit responses. These results shown that wideband phase shifter MMIC circuits with good performances can be achieved using the described method.

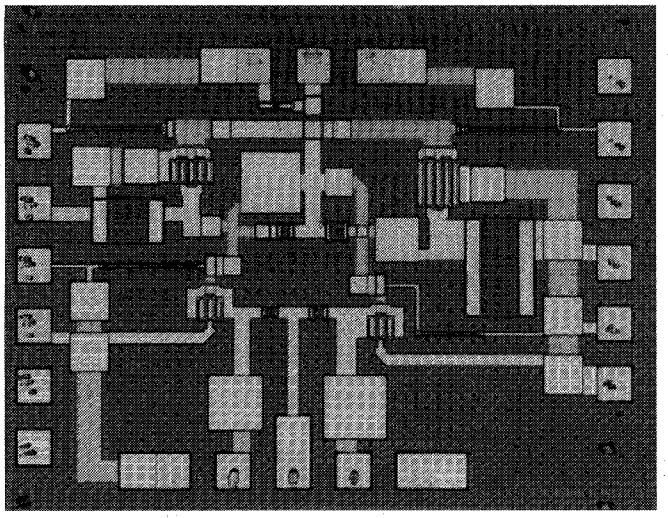

Fig. 15. Chip photograph.

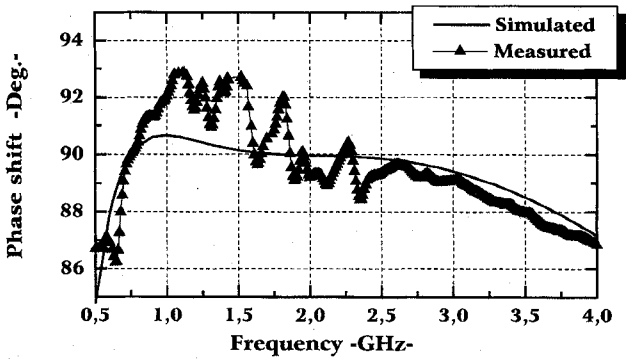

Fig. 16. Phase shift between output terminals.

APPENDIX A
PHASE DIFFERENCE MAXIMUMS COMPUTATION

The phase difference expression is rewritten as

$$\tan\left(\frac{\Phi(f)}{2}\right) = \frac{\frac{1}{Q_0}\left(r-\frac{1}{r}\right)\left(\frac{f}{f_0}+\frac{f_0}{f}\right)}{\frac{1}{Q_0^2}-\left(r-\frac{1}{r}\right)^2-4+\left(\frac{f}{f_0}+\frac{f_0}{f}\right)^2} \quad \text{(A1)}$$

the above expression is derived with respect to the variable $(\frac{f}{f_0}+\frac{f_0}{f})$ as follows:

$$\frac{d\left(\tan\left(\frac{\Phi}{2}\right)\right)}{d\left(\frac{f}{f_0}+\frac{f_0}{f}\right)} = \frac{\frac{1}{Q_0}\left(r-\frac{1}{r}\right)\left\{\left(\frac{f}{f_0}+\frac{f_0}{f}\right)^2-\left[\frac{1}{Q_0^2}-\left(r-\frac{1}{r}\right)^2-4\right]\right\}}{\left[\frac{1}{Q_0^2}-\left(r-\frac{1}{r}\right)^2-4+\left(\frac{f}{f_0}+\frac{f_0}{f}\right)^2\right]^2} \quad \text{(A2)}$$

the two maximums occur at the frequencies $f_{m1,2}$ given by the followings equation

$$\left(\frac{f_m}{f_0}+\frac{f_0}{f_m}\right)^2 = \frac{1}{Q_0^2}-\left(r-\frac{1}{r}\right)^2-4 \quad \text{(A3)}$$

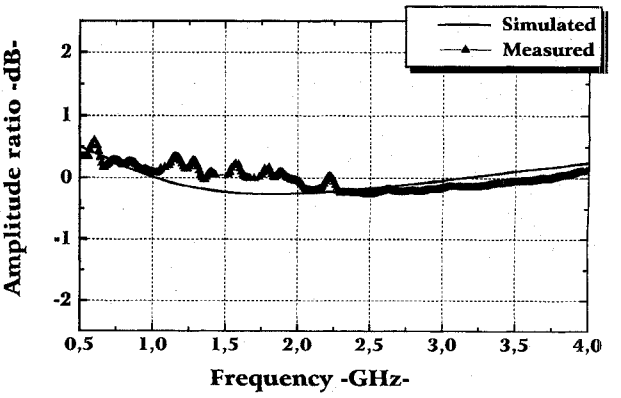

Fig. 17. Amplitude ratio between output terminals.

replacing the variable $(\frac{f}{f_0}+\frac{f_0}{f})$ in (A1) by (A3) we get the maximums expression

$$\Phi_{\max} = 2\cdot\tan^{-1}\left\{\frac{1}{2}\frac{1}{Q_0}\left(r-\frac{1}{r}\right)\times\left[\frac{1}{Q_0^2}-\left(r-\frac{1}{r}\right)^2-4\right]^{-\frac{1}{2}}\right\}. \quad \text{(A4)}$$

REFERENCES

[1] H. Kamitsuna and H. Ogawa, "Ultra-wideband MMIC active power splitters with arbitray phase relationships," *IEEE Trans. Microwave Theory Tech.*, vol. 41, no. 9, pp. 1519–1523, Sept. 1993.

[2] Y. Deville, "GaAs active structures with applications to microwave wideband 90° phase shifters," *Int. J. Electron.*, vol. 70, no. 1, pp. 201–211, 1991.

[3] S. K. Altes, T.-H. Chen, and L. J. Ragonese, "Monolithic RC all-pass networks with constant-phase-difference outputs," *IEEE Trans. Microwave Theory Tech.*, vol. MTT-34, no. 12, pp. 1533–1537, Dec. 1986.

[4] J. I. Alonso *et al.*, "GaAs MMIC wide band 4-way phase splitter," in *Proc. 22nd European Microwave Conf.*, Madrid, Spain, Sept. 1993, pp. 840–842.

[5] S. T. Salvage, R. J. Hash, and B. E. Petted, "An octave band GaAs analog phase shifter," in *Proc. IEEE MTT-S Int. Microwave Symp.*, June 1989, pp. 1051–1054.

[6] D. E. Norgaard, "The phase-shift method of single-sideband signal generation," in *Proc. I.R.E*, Dec. 1956, vol. 44, no. 12, pp. 1718–1735.

[7] P. A. Baker, "Phase-modulation data sets for serial transmission at 2000 and 2400 bits per second," *AIEE Commun. Tech.*, pp. 166–171, July 1962.

[8] K. Yamamoto *et al.*, "A 1.9 GHz-band GaAs direct-quadrature modulator IC with a phase shifter," *IEEE J. Solid-State Circuits*, vol. 28, no. 10, pp. 994–1000, Oct. 1993.

[9] A. Bóveda, F. Ortigoso, and J. I. Alonso, "A 0.7–3 GHz GaAs QPSK/QAM direct modulator," *IEEE J. Solid-State Circuits*, vol. 28, no. 12, pp. 1340–1349, Dec. 1993.

[10] A. Angelucci *et al.*, "Wideband phase control in mobile-radio antenna beamforming," in *Proc. Asia-Pacific Microwave Conf., APMC'94*, Tokyo, Japan, Dec. 6–9, pp. 105–108.

[11] D. G. Luck, "Properties of some wide-band phase splitting networks," in *Proc. IRE*, Feb. 1949, pp. 147–151.

[12] D. K. Weaver, "Design of RC wide-band 90° phase difference networks," in *Proc. IRE*, Apr. 1954, vol. 42, no. 4, pp. 671–676.

[13] W. Saraga, "The design of wide-band phase splitting networks," in *Proc. IRE*, July 1950, vol. 38, no. 7, pp. 754–770.

[14] S. D. Bedrosian, "Normalized design of 90° phase-difference networks," *IRE Trans. Circuit Theory*, vol. CT-7, pp. 128–136, June 1960.

[15] W. J. Albersheim *et al.*, "Computation methods for broad-band 90° phase difference networks," *IEEE Trans. Circuit Theory*, vol. CT-16, no. 2, pp. 189–169, May 1969.

Mustapha Mahfoudi was born in Kebdana, Morocco, in 1966. He received the degree in physics (electronics branch) from the Abdelmalek Saadi University, Tetouan, Marocco, in 1990. He is currently a Ph.D. student at Signals, Systems and Radiocommunications Department at the Technical School of Telecommunication Engineering of Polytechnic University of Madrid, Spain.

He has been engaged in research and development of MMIC circuits for active array antennas and digital radio links.

José I. Alonso (M'94) was born in Villacañas (Toledo), Spain. He received the degree in telecommunication engineering in 1982 and the Ph.D. degree in 1989, both from the Polytechnic University of Madrid, Spain.

From 1982 to 1985 he worked as a Microwave Design Engineer at Telettra España S.A./Alcatel Standard S.A. In 1985, he joined Signals, Systems and Radiocommunications Department at the Technical School of Telecommunication Engineering, where he is currently Associate Professor. His research is concerned with computer-aided design of high-speed/high-frequency integrated circuits and their interconnections. In addition, he has been engaged in research and development on GaAs monolithic integrated microwave circuits (MMIC's) and their applications to mobile, satellite, and optical-fiber comunications systems.